

## Comparison of the $k \cdot p$ and the direct diagonalization approaches for describing the electronic structure of quantum dots

Huaxiang Fu, Lin-Wang Wang, and Alex Zunger

Citation: [Applied Physics Letters](#) **71**, 3433 (1997); doi: 10.1063/1.120421

View online: <http://dx.doi.org/10.1063/1.120421>

View Table of Contents: <http://scitation.aip.org/content/aip/journal/apl/71/23?ver=pdfcov>

Published by the [AIP Publishing](#)

---

### Articles you may be interested in

[Electronic structure and optical gain saturation of  \$\text{InAs}\_{1-x}\text{N}\_x/\text{GaAs}\$  quantum dots](#)

*J. Appl. Phys.* **105**, 123705 (2009); 10.1063/1.3143025

[An atomistic-based correction of the effective-mass approach for investigating quantum dots](#)

*J. Appl. Phys.* **104**, 104309 (2008); 10.1063/1.3021059

[Comparison of the  \$k \cdot p\$  and direct diagonalization approaches to the electronic structure of  \$\text{InAs}/\text{GaAs}\$  quantum dots](#)

*Appl. Phys. Lett.* **76**, 339 (2000); 10.1063/1.125747

[Response to "Comment on 'Comparison of the  \$k \cdot p\$  and the direct diagonalization approaches for describing the electronic structure of quantum dots'" \[\*Appl. Phys. Lett.\* \*\*73\*\*, 1155 \(1998\)\]](#)

*Appl. Phys. Lett.* **73**, 1157 (1998); 10.1063/1.122155

[Comment on "Comparison of the  \$k \cdot p\$  and the direct diagonalization approaches for describing the electron structure of quantum dots" \[\*Appl. Phys. Lett.\* \*\*71\*\*, 3433 \(1997\)\]](#)

*Appl. Phys. Lett.* **73**, 1155 (1998); 10.1063/1.122114

---

A promotional banner for COMSOL software. On the left, a white box contains the text 'LIVE DEMO' and 'The Basics of COMSOL in 18 Minutes'. On the right, a blue button says 'REGISTER >>'. The background features a 3D model of a quantum dot structure with colorful streamlines representing electron transport or wave functions. The COMSOL logo is in the bottom left corner.

LIVE DEMO

# The Basics of COMSOL in 18 Minutes

REGISTER >>

COMSOL

# Comparison of the $k \cdot p$ and the direct diagonalization approaches for describing the electronic structure of quantum dots

Huaxiang Fu, Lin-Wang Wang, and Alex Zunger<sup>a)</sup>  
National Renewable Energy Laboratory, Golden, Colorado 80401

(Received 11 August 1997; accepted for publication 4 October 1997)

It is shown that the standard (decoupled)  $6 \times 6 k \cdot p$  effective-mass approach for semiconductor quantum dots overestimates significantly the hole and electron confinement energies, and, for dots made of materials with small spin-orbit coupling (e.g., phosphides, sulphides) produces a reverse order of  $s$ - and  $p$ -like valence states. By contrasting the electronic structures of dots as obtained by a direct diagonalization (multiband) pseudopotential approach and by its  $k \cdot p$  approximation, we are able to trace the systematic errors of  $k \cdot p$  in dots to the  $k \cdot p$  errors in the underlying bulk solids. This suggests a “diagnostic tool” and a strategy for improving the  $k \cdot p$ . © 1997 American Institute of Physics. [S0003-6951(97)00449-X]

It is now possible to produce via techniques of colloidal chemistry<sup>1</sup> nearly spherical quantum dots of a variety of semiconductor materials (CdSe,<sup>2,3</sup> InP,<sup>4</sup> InAs,<sup>5</sup> Si<sup>6</sup>), with typical diameters of 30–60 Å and good surface passivation. The rich spectroscopy<sup>2–5</sup> of such dots has been analyzed, almost universally, using a theoretical model that is so common that we term it the “standard model.” This “ $k \cdot p$  effective mass approach,”<sup>3,5,7–12</sup> expands the wave functions of the dot in terms of a linear combination of  $N_b$  bulk Bloch functions at the Brillouin zone center ( $\mathbf{k}=0$ , or  $\Gamma$  point). The most sophisticated version applied widely to quantum dots is<sup>3,5,9,10</sup> the  $6 \times 6 k \cdot p$  (i.e.,  $N_b=6$ ). We know, however, that the loss of translational periodicity in all three dimensions could lead in a quantum dot to coupling between many ( $N_b \gg 1$ ) bulk bands, and that this coupling could extend in momentum space well beyond the Brillouin zone center. This physical need for a large number of bulk basis functions is mitigated in the (small basis  $N_b \approx 6$ ) standard model by the introduction of empirical matrix elements (“Luttinger parameters”) drawn from the corresponding bulk solid. The rapid increase in the number of such energy parameters as the basis size  $N_b$  increases, and the fact that some of the parameters are not physical observables, limit one’s ability to improve the standard model by raising  $N_b$  systematically. Thus, the model itself does not provide an intrinsic, reflective mechanism for judging when more bands and more parameters are needed to correctly describe a given quantum dot system.

We have recently developed an alternative theoretical approach<sup>13–15</sup> that includes, at the outset, a converged number of bands without the need to introduce redundant empirical parameters. We solve via direct diagonalization (DD) the single particle Schrodinger equation

$$\left\{ -\frac{1}{2} \nabla^2 + \sum_n \sum_\alpha v_\alpha(\mathbf{r} - \mathbf{R}_n - \mathbf{d}_\alpha) \right\} \psi^{(i)} = \epsilon \psi^{(i)}, \quad (1)$$

where  $v_\alpha(r)$  is the screened nonlocal pseudopotential of atom of type  $\alpha$  (both the dot material and its passivating layer) located at “cell”  $n$  and site  $\mathbf{d}_\alpha$ . This pseudopotential is derived<sup>14</sup> from *ab initio* local density approximation

(LDA) calculations on the underlying bulk solid and includes adjustments to correct the LDA error in bulk band energies. The wavefunctions  $\psi^{(i)}$  are expanded in a plane wave basis, and matrix elements of  $v_\alpha$  are computed essentially exactly via numerical Fourier transformation. For periodic bulk solids, Eq. (1) is solved using conventional matrix diagonalization techniques. This produces the Bloch function  $\psi_{n\mathbf{k}}(\mathbf{r}) = e^{i\mathbf{k} \cdot \mathbf{r}} u_{n\mathbf{k}}(\mathbf{r})$  of band  $n$  and wavevector  $\mathbf{k}$ , and the bulk band structure dispersion  $\epsilon_{n\mathbf{k}}$ .

For  $\sim 10^3$ -atom quantum dot, conventional diagonalization techniques are impractical, so we solved Eq. (1) via the novel “folded spectrum method” (FSM),<sup>15</sup> that provides exact eigen solutions of the near-edge states at a computational cost that increases only linearly with the system’s size. Unlike the standard model, surface effects are treated explicitly and effective mass approximations are not invoked. Unlike tight-binding model,<sup>16</sup> the dot wavefunctions  $\psi(\mathbf{r})$  are known explicitly, and a variationally flexible basis set is used. Our method was previously applied to nanostructures of Si,<sup>13</sup> CdSe,<sup>17,18</sup> GaAs,<sup>18</sup> and InP.<sup>19</sup> We propose to use here this direct diagonalization approach to analyze the  $k \cdot p$  approach. Specifically, we will start from a given atomic pseudopotential  $\{v_\alpha\}$  for InP and draw from it the electronic structure of spherical InP quantum dots as obtained, in parallel, via the  $6 \times 6 k \cdot p$  and by direct diagonalization. Given the physically equivalent inputs, differences and similarities in the ensuing electronic structure will then be directly analyzable in terms of the basis set representation used by the two approaches. This will give us a new “diagnostic tool” for analyzing when the standard model is adequate and what aspect, specifically, needs to be corrected for a given system.

In the  $k \cdot p$  approach,<sup>7,8</sup> the wave functions of the dot are expanded by  $N_b$  zone-center Bloch functions

$$\psi^{(i)}(\mathbf{r}) = \sum_n \left\{ \sum_{\mathbf{k}} b_n^{(i)}(\mathbf{k}) e^{i\mathbf{k} \cdot \mathbf{r}} \right\} u_{n,\mathbf{k}=0}(\mathbf{r}). \quad (2)$$

In practical applications to large gap quantum dots,<sup>3,9,10</sup> one decouples the valence bands from the conduction bands, and treats the latter by a  $2 \times 2$  model<sup>11</sup> while describing the former by a  $6 \times 6 k \cdot p$  model<sup>9,10</sup> using an isotropic mass approximation.<sup>12</sup> An infinite potential well is assumed here, although this restriction can be removed.<sup>3</sup> To perform  $k \cdot p$

<sup>a)</sup>Electronic mail: alex\_zunger@nrel.gov

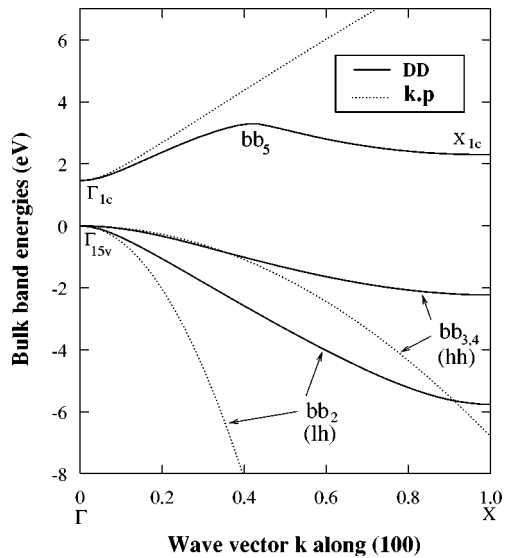


FIG. 1. Bulk band structure of zincblende InP as calculated by direct diagonalization (DD) pseudopotential method and by the  $6 \times 6 k \cdot p$  (plus  $2 \times 2$  for conduction band). We assume  $\Delta_0=0$ .

calculations that are equivalent to our pseudopotential direct diagonalization method, we need to determine the Luttinger parameters from our pseudopotential. To do so, we first solve Eq. (1) via direct diagonalization, obtaining the bulk dispersion  $\epsilon_{n,\mathbf{k}}$  and the effective masses. For InP, we find that in the absence of spin-orbit coupling (i.e.,  $\Delta_0=0$ ),  $m_{hh}(001)=0.474$ ,  $m_{hh}(111)=1.030$ ,  $m_{lh}(001)=0.097$ ,  $m_{lh}(111)=0.083$ , which are close to the experimentally observed values.<sup>14</sup> These anisotropic masses are used to derive, for  $\Delta_0=0$ , the (anisotropic) Luttinger parameters  $\gamma_1$ ,  $\gamma_2$ , and  $\gamma_3$ , which yield, after averaging, the pseudopotential-derived isotropic Luttinger parameters  $\gamma_1=4.86$  and  $\bar{\gamma}_2=1.66$  for the  $6 \times 6 k \cdot p$  model.

Figure 1 compares the exact dispersion  $\epsilon_{n,\mathbf{k}}$  (solid lines) with its  $6 \times 6 k \cdot p$  approximation  $\epsilon_{n,\mathbf{k}}^{k \cdot p}$  (dotted lines) for bulk periodic zinc-blende InP with lattice constant  $a=5.83 \text{ \AA}$  and spin-orbit parameter  $\Delta_0=0$ . We see that (i) near  $\Gamma$  the two methods produce identical results, by construction. (ii) The light-hole-like  $k \cdot p$  band (denoted  $bb_2$ ) deviates significantly from the exact counterpart immediately outside the  $\Gamma$  point. (iii) The heavy-hole-like valence bands (denoted  $bb_{3,4}$ ) are similar out to 30% of the  $\Gamma$ - $X$  distance. Finally, (iv) the conduction band (denoted  $bb_5$ ), obtained from the  $2 \times 2 k \cdot p$  calculation, deviates significantly from the strongly non-parabolic exact conduction band.

Figure 2 compares the results of direct-diagonalization (solid lines) and  $6 \times 6 k \cdot p$  (dotted lines) for the orbital energies of spherical InP dots of different sizes. The  $k \cdot p$  equations for dots are solved via the spherical-wave representation of Sercel and Vahala,<sup>12</sup> but using a  $6 \times 6$  rather than a  $4 \times 4 k \cdot p$  model.

The striking feature of Fig. 2 is that the  $k \cdot p$  approach produces (i) an incorrect order of the valence states: the state of (envelope function)  $p$  symmetry is above that of  $s$  symmetry. This incorrect order was seen in other  $k \cdot p$  calculations of dots with small spin-orbit energies, e.g., in<sup>10</sup> CdS and in<sup>9</sup> InP. We find that inclusion of (electron-hole) Coulomb correction to the pseudopotential result does not re-

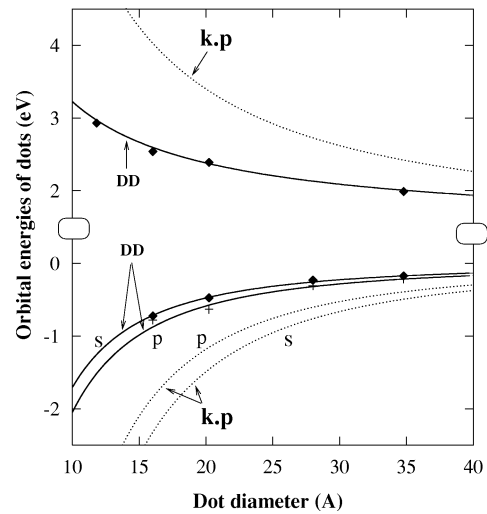


FIG. 2. Orbital energies of spherical, surface-passivated InP quantum dots as obtained by direct-diagonalization (DD) pseudopotential and by the  $k \cdot p$  approach with pseudopotential-derived Luttinger parameters. We assume  $\Delta_0=0$ .

verse the  $s/p$  order. Since the lowest dot conduction state always has  $s$  symmetry, the  $k \cdot p$  method predicts that the lowest transition ( $p \rightarrow s$ ) is forbidden in one-photon experiments and allowed in two-photon experiments, while a direct diagonalization predicts that the lowest transition ( $s \rightarrow s$ ) is one-photon allowed. (ii) The  $k \cdot p$  energy levels are considerably deeper (larger confinement) than the “exact” pseudopotential results. The latter give the band gaps versus sizes in good agreement with experiment.<sup>19</sup> For a dot with 20  $\text{\AA}$  diameter, the  $k \cdot p$  error for valence states is  $\sim 600 \text{ meV}$ , and (iii) the curvature of conduction energies versus size is considerably too large in  $k \cdot p$ . Unlike the enhanced (many-body) quasiparticle self-energy in local density functional calculation for Si dots,<sup>20</sup> the overestimated confinement energies of  $k \cdot p$  in Fig. 2 result from the improper  $k \cdot p$  bulk dispersion, i.e., from the one-body effect.

To analyze the reason for these discrepancies, we project the dot wave functions  $\psi^{(i)}(\mathbf{r})$  obtained from Eq. (1) onto the bulk Bloch wavefunctions  $\{\psi_{n,\mathbf{k}}(\mathbf{r})\}$ . Unlike the  $k \cdot p$  expansion Eq. (2), we do not limit the projection to just  $\mathbf{k}=0$ , but use

$$\psi_{\text{dot}}^{(i)}(\mathbf{r}) = \sum_n \sum_{\mathbf{k}} c_{n,\mathbf{k}}^{(i)} \{e^{i\mathbf{k} \cdot \mathbf{r}} u_{n,\mathbf{k}}(\mathbf{r})\}. \quad (3)$$

Figure 3 plots the spectral decomposition coefficients  $|c_{n,\mathbf{k}}^{(i)}|^2$  of the lowest conduction state [Fig. 3(a)] and the two highest valence states [i.e., with  $s$  (solid lines) and  $p$  (dotted lines) symmetries in Fig. 3(b)] of the InP dot with a diameter of 34.8  $\text{\AA}$ . We label the lowest eight bulk bands ( $bb_n$ ) by the index  $n$  with increasing energy order, as shown in Fig. 1. We see from Fig. 3 that:

(a) The  $s$ -like dot valence state has a large contribution from the bulk light-hole band ( $bb_2$ ), while the  $p$ -like dot valence state has no contribution from the bulk light-hole band. Given that the  $k \cdot p$  approximation places the bulk light-hole band at spuriously deep energies (Fig. 1), we expect that the  $k \cdot p$  will also place the dot’s  $s$ -like state at too

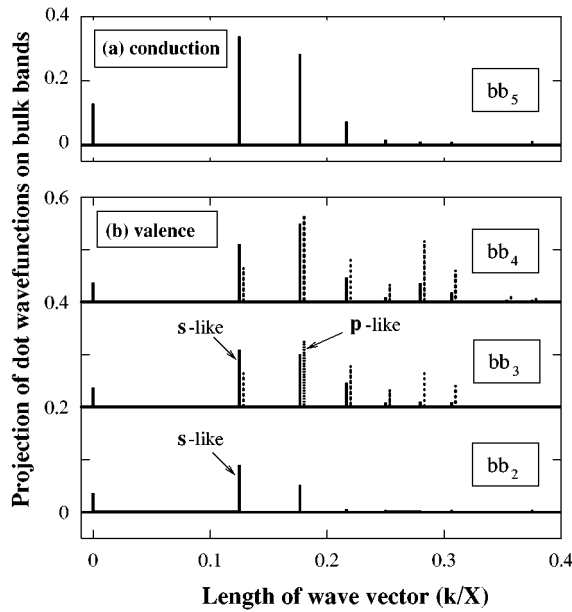


FIG. 3. Spectral coefficients  $|c_{n,\mathbf{k}}^{(i)}|^2$  [Eq. (3)] showing how much of the bulk bands  $|n\mathbf{k}\rangle$  participates in each state  $|i\rangle$  of the InP dot with diameter 34.8 Å. The bulk bands ( $bb_n$ ) are marked in increasing order of energy (see Fig. 1), where  $bb_2$  is light hole-like,  $bb_{3,4}$  are heavy hole-like, and  $bb_5$  is bulk conduction band. *s*-like states: solid lines. *p*-like states: dotted lines.

deep an energy (over confinement). This is indeed borne out by Fig. 2.

(b) The *s*-like dot valence band has a significant contribution from  $\Gamma$  point ( $\mathbf{k}=0$ ), whereas the *p*-like dot valence state has no contribution from  $\mathbf{k}=0$ . Also, the  $\mathbf{k}$  points which contribute most significantly to the dot *p*-like state are generally more distant from  $\mathbf{k}=0$  than those  $\mathbf{k}$  points which contribute significantly to the dot *s*-like state. Given that the *k*·*p* approach does not describe well the bulk dispersion away from  $\Gamma$  (Fig. 1), we expect that the *k*·*p* model will not describe the *p*-like dot valence state well either. This is also borne out by Fig. 2.

(c) The *s*-like dot valence state has a larger contribution from the bulk conduction band than the *p*-like dot valence state, indicating that the *s*-like dot valence state is more affected by the neglect of coupling with the conduction bands in the standard *k*·*p* model. Effects (a)–(c) explain why the  $6\times 6$  *k*·*p* produces an incorrect order of *s* and *p* valence states while over estimating the global confinement.

(d) The lowest *s*-like dot conduction state has a large contribution from the lowest bulk conduction band away from the  $\mathbf{k}=0$  zone center. Since the *k*·*p* overestimates significantly the up dispersion of the bulk conduction band (Fig. 1), we expect it also to over estimate the dot's conduction state energy. This is indeed borne out by our direct calculation (Fig. 2).

The above arguments can be quantified. We can approximately model the orbital energies of the *dot* as a linear combination of the orbital energies of the underlying *bulk*, using our spectral coefficients of Eq. (3) as weights:

$$\bar{\epsilon}_i^{\text{dot}} = \sum_n \sum_{\mathbf{k}} \epsilon_{n,\mathbf{k}}^{\text{bulk}} |c_{n,\mathbf{k}}^{(i)}|^2. \quad (4)$$

The orbital energies of the *s*-, *p*-like valence states, and the lowest conduction state of the InP dot with 34.8 Å diameter as obtained by direct diagonalization are (in eV), respectively,  $(\epsilon_s, \epsilon_p, \epsilon_{cb}) = (-0.17, -0.22, +1.99)$  while *k*·*p* gives  $(\bar{\epsilon}_s^{k\cdot p}, \bar{\epsilon}_p^{k\cdot p}, \bar{\epsilon}_{cb}^{k\cdot p}) = (-0.49, -0.39, +2.42)$  with a reverse *s/p* order, as noted above. The model [Eq. (4)], using 16 (counting spin degeneracy) pseudopotential bulk bands, gives  $(\bar{\epsilon}_s, \bar{\epsilon}_p, \bar{\epsilon}_{cb}) = (-0.19, -0.24, +2.01)$ , which are quite close to the results obtained by direct diagonalization. The model also gives the correct *s/p* order. Thus, the six bulk bands used by *k*·*p* are not as potent as the 16 exact bands in portraying the dot's states.

We conclude that the *k*·*p* errors in quantum dots can be diagnosed via the *k*·*p* errors in the corresponding bulk solids. Specifically, Figs. 1–3 show that the *k*·*p* method needs to primarily bend the bulk light hole band ( $bb_2$ ) upwards and to couple the bulk conduction with the valence bands in order to produce qualitatively correct electronic structure of spherical quantum dots. Since the  $6\times 6$  *k*·*p* produces errors even for a large-gap ( $\sim 2$  eV) dot material such as InP, inclusion of the conduction band (i.e., a  $8\times 8$  model) is not expected to lead to significant improvements, unless the lh band is fixed, at the same time.

This work was supported by the U.S. Department of Energy, OER-BES, under Grant No. DE-AC36-83CH10093.

- <sup>1</sup>A. Henglein, Chem. Rev. **89**, 1861 (1989).
- <sup>2</sup>M. Chamarro, C. Gourdon, P. Lavallard, O. Lublinskaya, and A. I. Ekimov, Phys. Rev. B **53**, 1336 (1996).
- <sup>3</sup>D. J. Norris and M. G. Bawendi, Phys. Rev. B **53**, 16 338 (1996).
- <sup>4</sup>O. I. Micic, J. Sprague, Z. Lu, and A. J. Nozik, Appl. Phys. Lett. **68**, 3150 (1996).
- <sup>5</sup>A. A. Guzelian, U. Banin, A. V. Kadavanich, X. Peng, and A. P. Alivisatos, Appl. Phys. Lett. **69**, 1432 (1996); U. Banin, J. C. Lee, A. A. Guzelian, and A. P. Alivisatos (unpublished).
- <sup>6</sup>L. E. Brus, J. Phys. Chem. **98**, 3575 (1994).
- <sup>7</sup>J. M. Luttinger and W. Kohn, Phys. Rev. **97**, 869 (1955).
- <sup>8</sup>E. O. Kane, in *Semiconductor and Semimetals*, edited by R. K. Willardson and A. C. Beer (Academic, New York, 1966), Vol. I, p. 75.
- <sup>9</sup>T. Richard, P. Lefebvre, H. Mathieu, and J. Allegre, Phys. Rev. B **53**, 7287 (1996).
- <sup>10</sup>G. B. Grigoryan, E. M. Kazaryan, Al. L. Efros, and T. V. Yazeva, Sov. Phys. Solid State **32**, 1031 (1990).
- <sup>11</sup>D. I. Chepic, Al. L. Efros, A. I. Ekimov, M. G. Ivanov, V. A. Kharchenko, I. A. Kudryavtsev, and T. V. Yazeva, J. Lumin. **47**, 113 (1990).
- <sup>12</sup>P. C. Sercel and K. J. Vahala, Phys. Rev. B **42**, 3690 (1990).
- <sup>13</sup>L. W. Wang and A. Zunger, in *Nanocrystalline Semiconductor Materials*, edited by P. V. Kamat and D. Meisel (Elsevier, Amsterdam, 1996), p. 161.
- <sup>14</sup>H. Fu and A. Zunger, Phys. Rev. B **55**, 1642 (1997); L. W. Wang and A. Zunger, Phys. Rev. B **51**, 17 398 (1995).
- <sup>15</sup>L. W. Wang and A. Zunger, J. Chem. Phys. **100**, 2394 (1994).
- <sup>16</sup>G. Allan, C. Delerue, and M. Lannoo, Phys. Rev. B **48**, 7951 (1993).
- <sup>17</sup>L. W. Wang and A. Zunger, Phys. Rev. B **53**, 9579 (1996).
- <sup>18</sup>A. Franceschetti and A. Zunger, Phys. Rev. Lett. **78**, 915 (1997).
- <sup>19</sup>H. Fu and A. Zunger, Phys. Rev. B **56**, 1496 (1997).
- <sup>20</sup>S. Ogut, J. R. Chelikowsky, and S. G. Louie, Phys. Rev. Lett. **79**, 1770 (1997).